GEOTHERMAL 3D SUBSURFACE MODELING A CASE STUDY FROM SORIK MARAPI FIELD, INDONESIA

A.C. Licup, Jr.[1], Z.F. Sarmiento[3], X.L. Omac[2], F.C. Maneja[2], V.R. Chandra[1], M.B. Esberto[2], M.J.Z. Villareal[2], A.S.J. Baltasar[2], S. Mulyani[4], P.P. Sari[4], Jhonny [4], D. Juandi[4]

[1]PT Sorik Marapi Geothermal Power, [2]FEDCO
[3]KS Orka Renewables PT Ltd, [4]Schlumberger

e-mail: armando.licup@ksorka.com; zammy.sarmiento@ksorka.com; omac.xl@gmail.com; felix_maneja06@yahoo.com; vicky.chandra@ksorka.com; mig.esberto@gmail.com; mjzvillareal@gmail.com; smulyani@slb.com; ppsari@slb.com; jjhonny@slb.com; djuandi@slb.com

ABSTRACT

Indonesia is considered to have the largest geothermal potential in the world, estimated at 29,000 MW and distributed from high, medium and low enthalpy geothermal systems. To date, only less than 5% have been utilized, but many other geothermal concessions are being developed and offered for further exploration and development. The Sorik Marapi geothermal field has been recently drilled with results indicating the existence of a high temperature-neutral resource. Maximum temperature measured so far has been recorded as 290°C, with three wells currently tested and producing an average of 11.5 MW.

Initial modeling works in the field has been completed and discussed in FEDCO (2017) NORC report paving the way forward for a strategy that prioritizes the development of the Sibanggor area. This paper deals with the 3D modeling studies conducted in the geothermal field, based on available data from surface exploration (3G-geological, geochemical and geophysical) surveys, and shallow and deep drilling in the 4 identified prospect areas. The 3D modeling utilizes Petrel® software from Schlumberger which allows interfacing of limited and non-standard data formats for easy and fast processing. The 3D model is structured to integrate the structural model, lithology and alteration zone, the 3D MT resistivity model and the temperature distribution collected from the 6 wells in the area.

The workflow in the models starts with data loading and quality control, creation of structural framework for fault modeling and generating 3D grid for reservoir property modeling to capture the lithology, resistivity and temperature distribution. Special workaround algorithms are required to ensure correct data loading. The final result of this study is the 3D subsurface static model defining the vertical and lateral resource boundaries as well as the prime resource areas which would be the basis of designing future well targets to achieve the targeted 240 MW installed capacity in the field. The same model would then be expanded in constructing the numerical model to match the natural state condition of the resource, and subsequently for making forecasts on the future reservoir behavior at different operating conditions.

Keywords: 3D subsurface model, structural, lithology, resistivity and temperature model, Petrel, Sorik Marapi, Indonesia

INTRODUCTION

The Sorik Marapi geothermal field is one of the liquid dominated systems located along the Great Sumatran Fault System (SFS). Several surface exploration works have been undertaken to characterize the field's geothermal potential. These include geophysical surveys, geochemical sampling and structural mapping based on LiDAR image interpretations. Now on its exploration drilling and early development stage, SMGP recently completed its first few production wells. To better visualize the field, both surface and subsurface geoscientific data obtained were utilized to develop various 3D models using Petrel® software. The output of this project consist of a 3D structural and lithological model of SMGP, as well as resistivity and temperature distribution in the field.

The model boundary used in this project is shown in Figure 1, encompassing the entire SMGP geothermal concession.

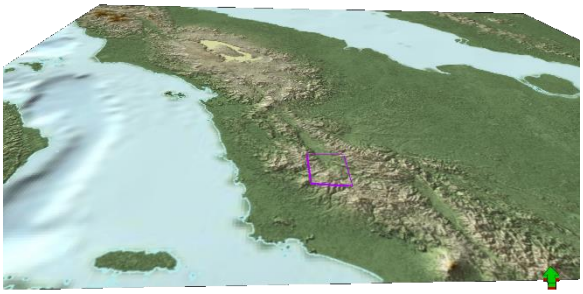

Figure 1: Model boundary location (purple square) at area study Sorik Marapi

REGIONAL GEOLOGY AND TECTONIC SETTING

Structural Geology

The Sumatran Fault System (SFS) is a long right-lateral strike-slip fault which traverses the entire length of the Sumatra Island. This zone of active deformation is attributed to the subduction within the Sunda Trench. The geomorphology of the SFS was found to be highly segmented, consisting of second order geometrical irregularities which splits the fault extent to at least nineteen (19) segments (Sieh and Natawidjaja, 2000). Such irregularity and an important tectonic feature of the SFS lie on the equator (between 0.1°S and 1.5°N), coined as the "*equatorial bifurcation*", where the fault splays to

two sub-parallel structures – Angkola and Baruman segments, with a widest separation of 35km at 0.7°N (Figure 2). This is known as the Panyabungan pull-apart basin, one of the thirteen (13) pull-apart basins mapped along the extent of the SFS (Muroaka et al., 2010). The SFS runs the length of the Barisan Mountains in Sumatra, the volcanic arc related to the Sunda trench. The Barisan Mountain is comprised of at least thirty-five (35) volcanoes, one of which is the active strato-volcano – Sorik Marapi (2,145 masl).

Stratigraphy

The stratigraphic units in the SMGP may be summarized into four (4) formations. From oldest to youngest, these are: (1) The ***Basement*** consisting of Mesozoic to Paleozoic metasediments (including shale and limestone), which are possibly intruded by plutonic rocks (including granodiorite and quartz diorite) (SKM, 2011), this unit has not been intercepted in the subsurface, thus far; (2) The ***Sibanggor Volcanic,*** formerly referred to as Old Volcanics, possibly of Tertiary Age, consisting of undifferentiated generally altered volcanics / volcaniclastics units with hardly distinguishable original composition and fabrics; (3) ***Roburan Volcanics***, predominantly dacitic to andesitic exhibiting pumiceous and porous texture with common primary micas; and (4) ***Sorik Marapi Volcanics***, consisted of young andesitic to basaltic lava flows and pyroclastic deposits that radiate outwards from the active Sorik Marapi volcano. Shown in Figure 3 is the stratigraphic cross-section of these formations as encountered in SMGP wells.

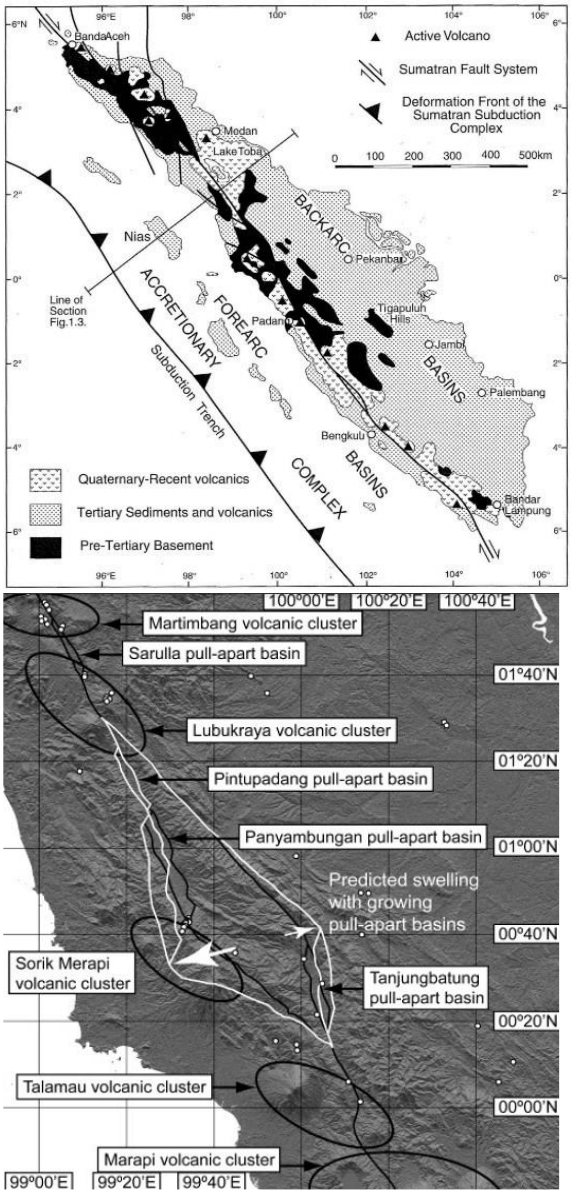

Figure 2: Volcano-tectonic setting of Sorik Marapi showing localized fault stresses in response to the dextral movement along the Sumatran Fault System (adapted from Muraoka, et al., 2010)

.

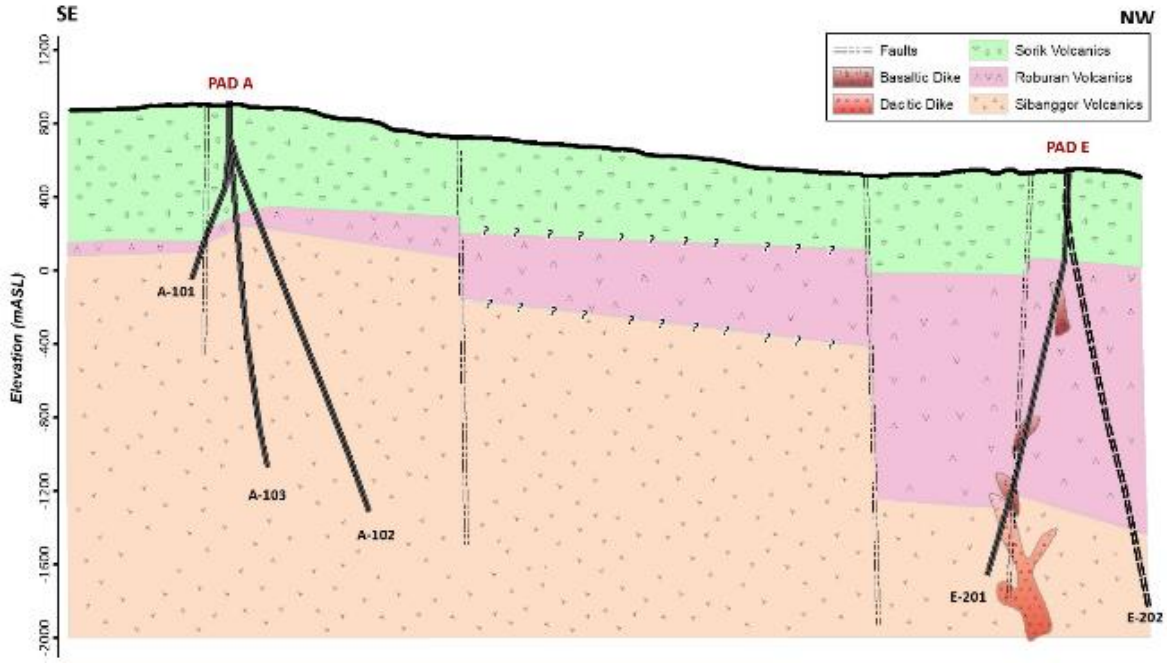

Figure 3: Stratigraphic Cross section based on encountered lithology among SMGP wells

Hydrothermal Alteration

The dominant alteration mineral assemblage of wells drilled in PAD A exemplified an alteration suite largely resulting from neutral pH geothermal fluids. At shallow levels (surface to 50masl), the alteration assemblage is composed of silica + chlorite + smectite + calcite ± iron oxides ± pyrite, which comprise the argillic zone or clay cap of the reservoir. The presence of common bladed calcite in Pad A wells at around +100 to +500masl insinuates boiling condition along these depths. At deeper levels, neutral to alkaline environment remain evident with the noted presence of rare secondary amphiboles, epidote and wairakite suggesting a formation temperature in excess of 250ºC. The ubiquitous presence of calcite suggests neutral pH fluids with high CO_2 fugacity which hinders the growth of epidote even at high temperatures.

On the other hand, Pad E wells showed a hydrothermal alteration assemblage that is lower in rank as compared to Pad A wells. Moreover, the clay zone is thicker in two Roburan wells where smectite persisted down to -930m msl. The abundance of Fe oxides throughout these wells suggest that the volcanic formation may have been deposited in a water-lain environment. Based on alteration mineralogy, predicted temperatures from E series wells may reach 220°C, which is relatively lower than A series wells.

GEOTHERMAL SYSTEM

The Upflow Zone

Previous studies conducted in Sorik Marapi have suggested varying conceptual models of the geothermal resource. SKM (2011) proposed that there are four (4) separate upflow zones in the project based on several MT resistivity anomalies. FEDCO (2016, 2017) favored a typical single geothermal system with an upflow zone that is associated and located near or directly beneath Mt. Sorik Marapi volcano. This interpretation is shared by ISOR (2016) in their due diligence study report for the area. This model is depicted with the main resource centered between Sorik Marapi and Sibanggor Tonga and overlain by a low resistivity layer. In view of the lack of MT data at Mt Sorik Marapi, a more definite shape and size of the upflow zone cannot be ascertained. However, such resistivity structure provides a good indication on the location of the nearest upflow zone. Recent drilling in Pad A confirmed the existence of hot geothermal fluids in Resource Area 1 in Sibanggor sector.

Two-phase Liquid Dominated System

Figure 4 shows the updated integrated conceptual model of Sorik Marapi geothermal resource (Fedco, 2017). It shows that mixtures of fluids and magmatic gases ascend vertically to the summit of Mt. Sorik and from there discharges magmatic gases, highly saline fluids with very low pH. Part of the mixtures of fluids finds its way laterally and channeled through fractures or faults leading to the Sibanggor area and appear at the surface as thermal springs and fumaroles. As the fluids migrate, the acidic fluids interact with the rocks and the overlying aquifer forming a mature geothermal system with a neutral pH as manifested in the thermal springs. This is supported by stable isotope ($\delta^{18}O$ and δD) data showing that samples from fumarole condensates, except from the Mt. Sorik crater, lie to the left of the meteoric water line. Geochemical samples from Sibanggor Tonga insinuate that the fluids come from a source with a temperature of 280°C while Roburan samples indicate that they are secondary fluids from steam-heated groundwater.

The temperature distribution from the wells drilled in Pad A shows a broad isothermal section and slight reversal-like in SMA-102 at deeper levels, suggesting the northern part of Sibanggor area is probably at the periphery of the main thermal plume. As inferred from the trend of hydrothermal alteration and isotherms and interpretation of the MT data, it is likely that the deep, near-neutral pH geothermal resource in Sibanggor might be centered beneath the eastern slope of Sorik Marapi volcano.

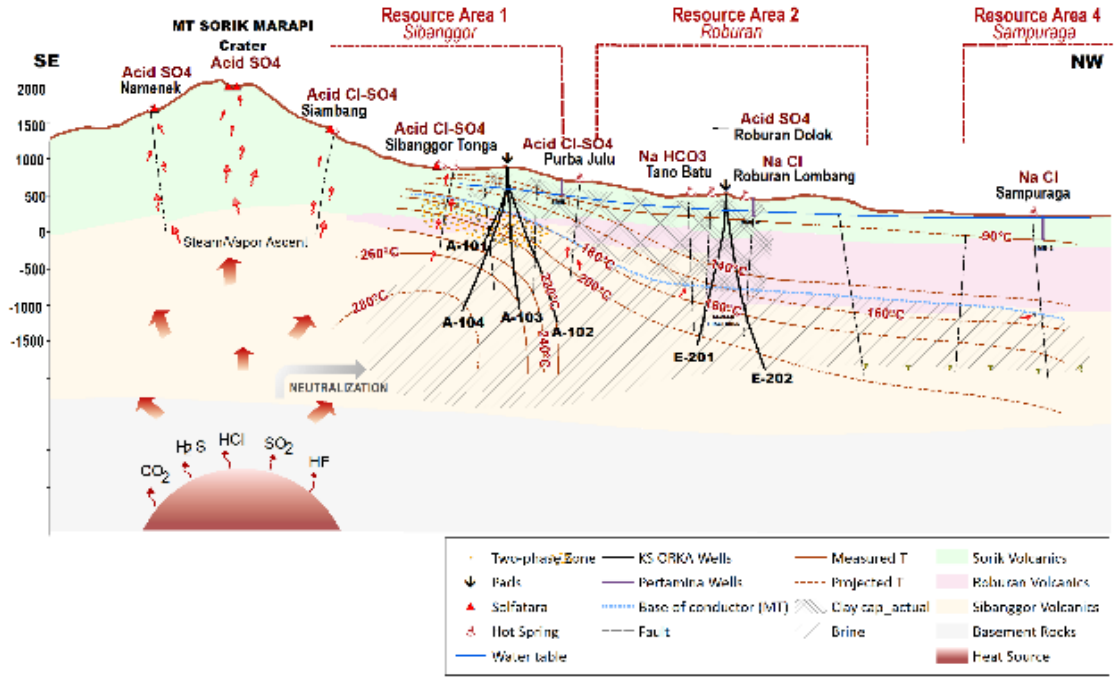

Figure 4: Updated Conceptual Model of the Sorik Marapi Geothermal Project

The benign nature of fluids tapped by Pad A wells has confirmed that the up flowing fluids have already undergone substantial neutralization. The main characteristic of this system is that a two-phase zone exists at the top of the main brine reservoir which was undoubtedly predicted even during the drilling stage due to the presence of common bladed calcite in all the wells from +100 to +500 mASL. All wells have temperature profiles falling within the boiling point for depth (BPD) curve from 100-200m MSL suggesting boiling condition at depth. Well SMA-103 exhibited highest temperature of 290°C at 1400m during shut condition.

The Cap Rock

The capping mechanism conspicuously differs between Pad A and Pad E wells. In Sibanggor sector, a comparatively thin conductive layer was recognized from MT survey. This can be correlated to the interpreted reservoir cap above +100m MSL among Pad A wells. The cap rock is characterized by widespread development of silica and interstitial calcite with generally minor smectite and interlayered clays. Fractures are hemmed in by amorphous quartz which are probably deposited due to pressure fluctuations as a consequence of episodic rupturing and silica sealing at the roof of the reservoir.

In Roburan sector, a thick conductive body was inferred through analysis of MT data. This roughly corresponds to predominant argillic alteration assemblage until -800m MSL. The conductive layer is made up of prevalent smectite, interlayered clays, iron hydroxides, amorphous silica and interstitial calcite. The extensive silica sealing at the base of cap rock was not observed in Pad E wells which suggests the lack or absence of hot fluid flow in the area in the recent past.

The Reservoir Host Rock

At the production section of Pad A wells (+100m to -1300m MSL), intensely altered rocks with hardly discernible original fabric and composition and exhibiting high-temperature alteration minerals are encountered. These rocks belong to the Sibanggor Formation where a general increase in well-formed secondary mineral crystals and abundant vein materials are observed specially within zones of fault intersections. The type of lithology, degree of alteration and existence of open fractures all indicate that this volcanic formation acts as the host for the geothermal reservoir. Reservoir temperatures exceeds 250°C as temperature gradient tends to increase towards the upflow zone.

On the other hand, Sibanggor Formation in Pad E wells was intersected deeper and are mostly altered to low and medium rank mineral assemblage and normally devoid of crystallinity. This further signify that Roburan sector is an impervious barrier that prevents vertical or lateral migration of geothermal fluids.

Outflow Zone

The signature of the outflowing fluids to the lowlands and possibly associated with the Mt. Sorik Marapi is exhibited by hot springs (96°C) in Sampuraga area, some 17 kilometers to the north of Sorik Marapi Crater (Figure 5). Whether Sampuraga is hydrologically connected with Sibanggor resource as suggested by geochemical data, it is not corroborated by the drilling results of wells SME-201 and SME-202. The steep thermal gradient from pad A to pad E, poor permeability and low hydrothermal alteration rank among pad E wells insinuate that Roburan sector is not part of the main lateral flow path from upflow region in Sibanggor en route to Sampuraga.

If there is some hydrological connection between Sampuraga and Sibanggor, the path should pass in area outside the low-lying corridor that stretches from Sibanggor to Roburan. A possible circuitous route would be through an area east of South Sumatran Marapi Central Fault. However, if this is true, well SMA-102 should be

very permeable and SME-202 should at least show some resemblance of alteration halo at depth.

Pursuing further the possibility of having hydrological connection between Sampuraga and Sibanggor, by some reckoning, is beneath the western mountain range. The limited MT resistivity data to the west provides a hint on this conjecture. Resistivity profiles has shown that there is possible domal MT resistivity structure west of Roburan which can be construed as possible flow of hot fluids. The solfataric activity at Roburan Dolok could just be a surface leak from that hydrological corridor. This mountain range is seemingly composed of volcanic chains that includes Sorik Marapi, an unnamed preserved crater and a cinder cone. An alternative explanation is that there is really no connection between Sampuraga and Sibanggor and they are actually separated by a cold block. This concept requires a heat source other than the Sibanggor upflow that supplies the hot geothermal fluids in Sampuraga. Figure 5 below shows location of volcanic centers within the mountain range that could be possible heat sources.

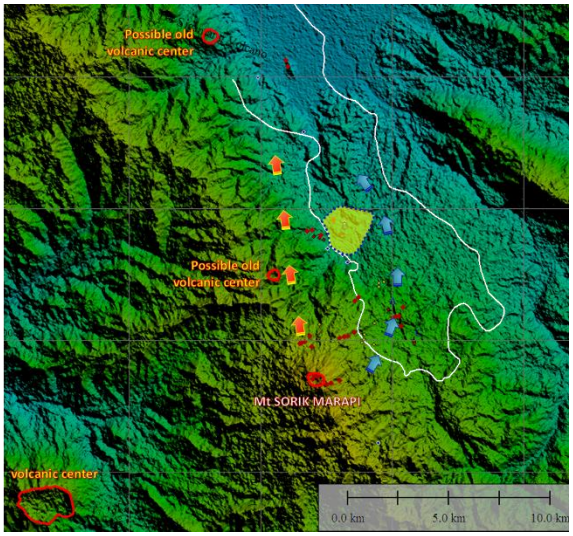

Figure 5: Interpreted outflow path from Mt. Sorik Marapi Upflow Zone to Sampuraga

DATA AND METHODOLOGY

Modeling process for the study area is done by updating the previous study which was created without well data. Several data from that study are still used for current modeling, they are fault polygons from surface mapping and LIDAR interpretation, 3D resistivity from magnetotelluric method and topography point data. There are 6 wells from 2 pad locations that are used as input data. The additional subsurface data consists of lithological information (cuttings), secondary mineral distribution, and temperatures at several depths (Figure 6).

The final model came from integration of those data. Structural model comprises of topography surface and fault planes which were generated from topography point data and fault polygons previously interpreted. On the other hand, lithology models were created based on cross sections of lithology facies from well data as shown at Figure 3. Supplementary lithological and alteration mineral data from wells have been used as additional information for this lithological model. Distribution model of resistivity value in the study area was extracted from 3D magnetotelluric points data (Figure 7).

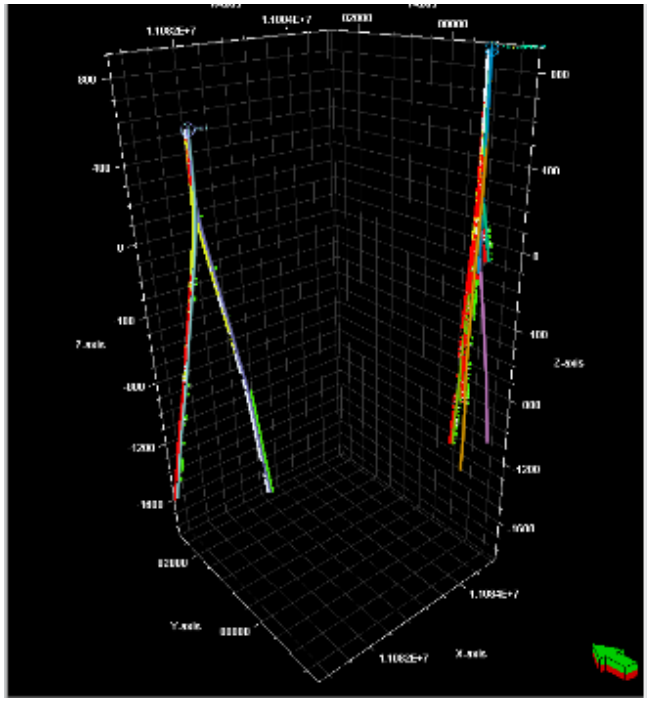

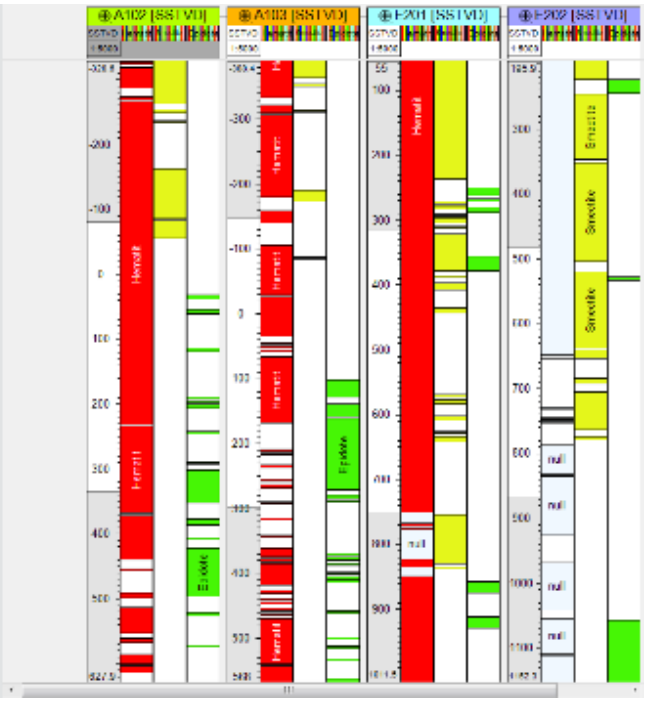

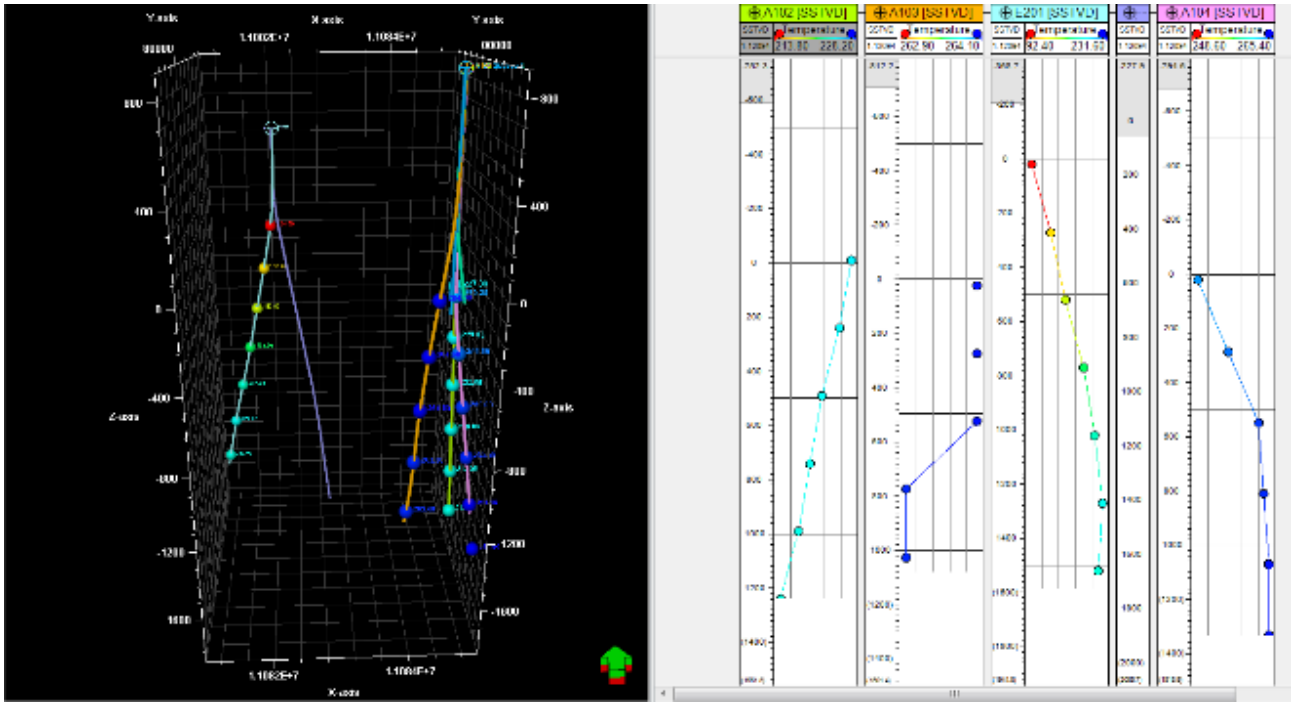

Figure 6: Additional information from well data including distribution of secondary minerals (above) and temperature at some depth (below)

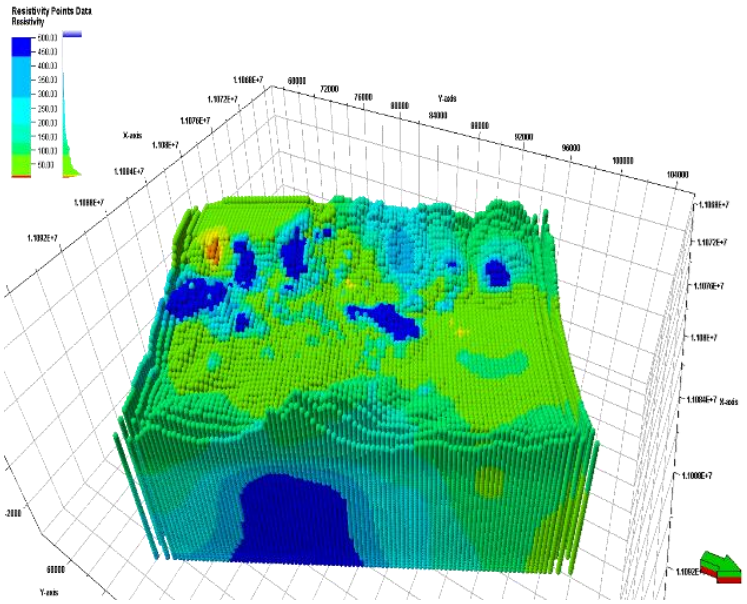

Figure 7: 3D resistivity MT point data for resistivity modeling (colors based on depth of points location)

The results of resistivity 3D models were also used as driver to populate the temperature values from well data to create 3D temperature model. Table 1 enumerates the data required for each modeling process.

Table 1: Data list for 3D subsurface modeling.

3D Models	Data
Structural	a. Topography point data b. Fault polygon from surface mapping
Lithology	a. Lithological data from wells b. Alteration minerals from wells c. Cross section of facies lithology
Resistivity	a. 3D Magneto telluric point data
Temperature	a. Measured well temperatures

The workflow for the 3D modeling of Sorik Marapi geothermal resource was adapted from similar study conducted in Aydin, Turkey, which used Petrel® as the modeling software (Akar, S. et al., 2011). Generally, there are four main steps in this workflow, they are: data input, structural modeling, property modeling, and Quality Check for the results (Figure 8).

Loading data into software are defined based on the files type. Topography, 3D resistivity and fault polygons were simply loaded as points and polygon. Lithology and temperature were imported as well data, while cross sections or map data were inputted as image. The Coordinate Reference System (CRS) was needed to make

sure all data are inputted correctly. This will influence the positions of data and the 3D visualizations. Structural modeling started by defining project boundaries that can cover all data and diversity. For this modeling process, a square polygon with and area of 7.4 x 10^8 m^2 was chosen as the lateral boundary. Then, surface map is gridded based on that boundary with topography point data as the main input. Topography condition of project area was represented by surface elevation map. The fault polygons were edited to enable them as input in fault framework. In this process, fault polygons that were expressed in the surface as 2D data has been transformed into fault planes which are 3D objects. There are 490 fault polygon data available for this project. In this case, fault data were classified into 4 classes based on LIDAR and surface evidences, they are either major or minor faults with high to medium confidences (Figure 9).

All fault planes can be modeled and used for a framework in the succeeding steps. However, modeling too many faults is a very tedious process and may result into unreasonably complicated 3D visuals. To simplify the approach, 73 fault planes were selected for the succeeding steps. Fault modeling defines the skeleton of 3D grid model and fault pillar based on selected fault planes. The skeleton will serve as guide for horizon modeling process to generate horizon data which represents the facies boundary. To get proper model, lithology cross section from well data has been used in the process. After that, zoning and layering were conducted to set the cell thickness. It is important to get more layers such that all point data will be captured into the 3D grid. When the 3D grid is ready, property modeling can now be performed. This process consists of geometrical modeling for lithology model, and petrophysical modeling for resistivity and temperature distributions. The final results of these models were verified by applying several methods such as creating cell volume to ensure that all cells at 3D grid model are correct, check the histogram for every result of petrophysical modeling, and view well section to validate the relationship between actual well data and results model

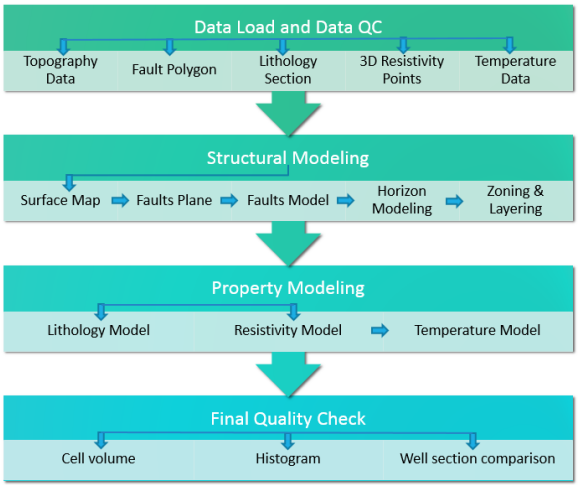

Figure 8: Workflow for 3D Subsurface Modeling using Petrel® software with four main stages: load data, structural, property modeling and final QC.

.

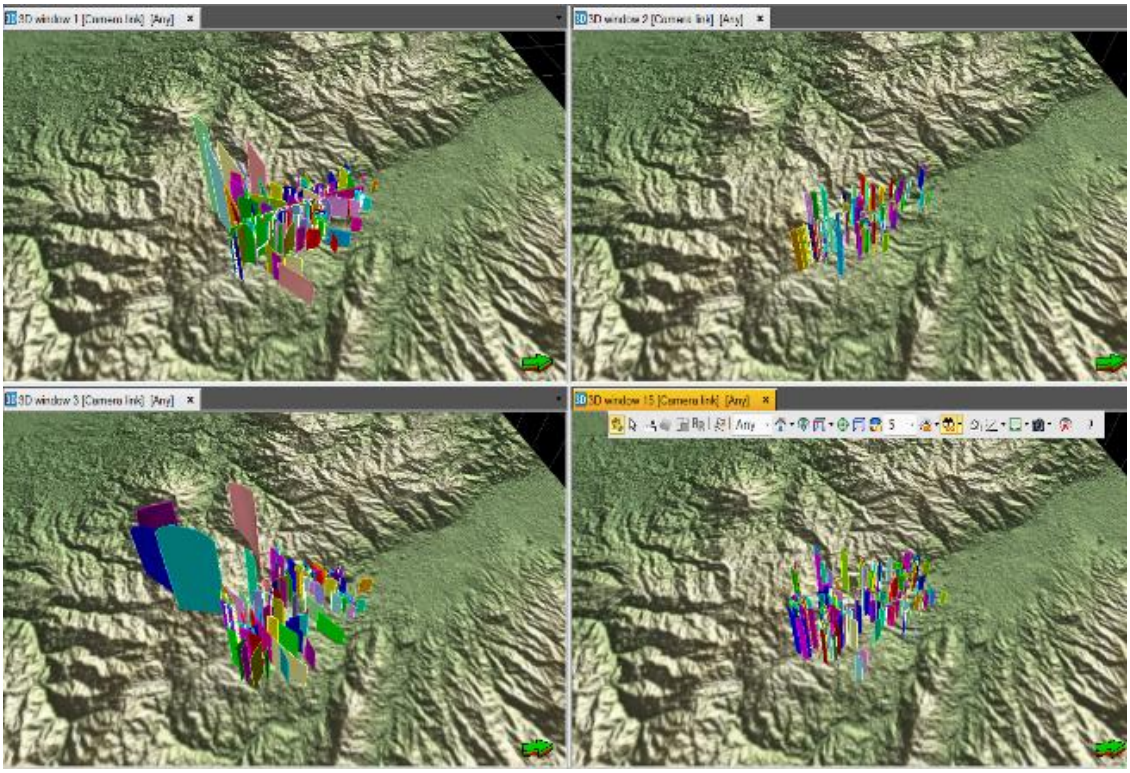

Figure 9: Faults plane data from faults polygon which classified into four classes: Major Minor faults with high confidence (1st row) and Major Minor faults with medium confidence (2nd row).

RESULTS MODEL

The final various 3D subsurface models of geothermal resource will be integrated to develop a single model. This comprises the fault model, the horizon model, and properties information such as lithology, resistivity and temperature. All of the results were created sequentially from structural fault model to property distribution in the 3D grid.

Structural and Lithological Models

The result of structural modeling is shown in Figure 10. Fault planes were modeled using process structural framework to 3D grid in Petrel®. Based on surface mapping and actual well-fault intersectio[illegible] were assigned with a dip range of 85º to [illegible] model demonstrated the complexity of structural framework in the project due to the movement along Sumatra Fault system and the formation of Panyabungan Graben. As more subsurface data become available, this model can be used in establishing the plumbing mechanism in SMGP.

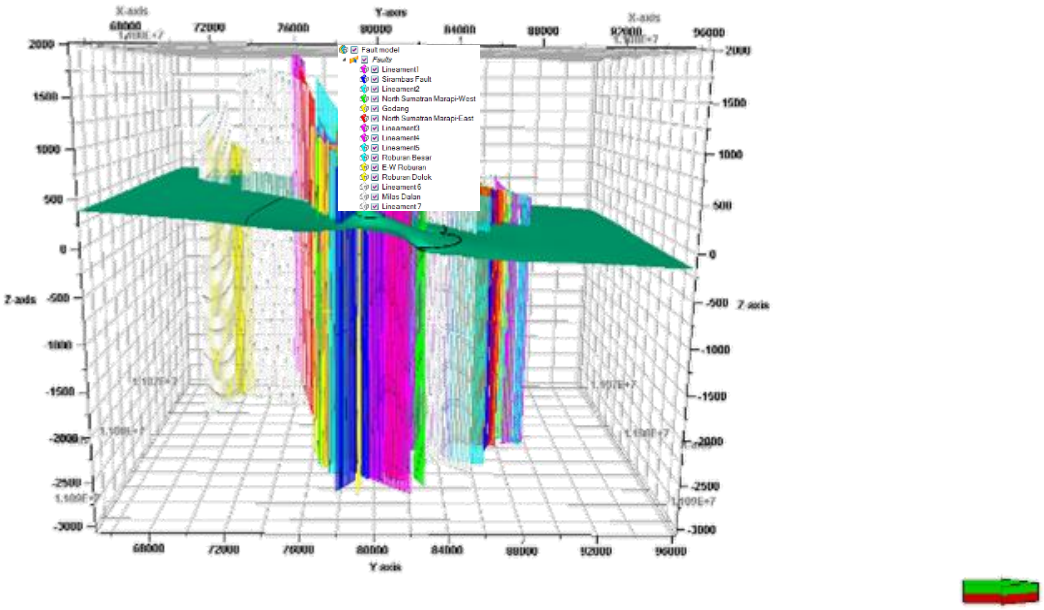

Figure 10: 3D Fault Modeling Subsurface results

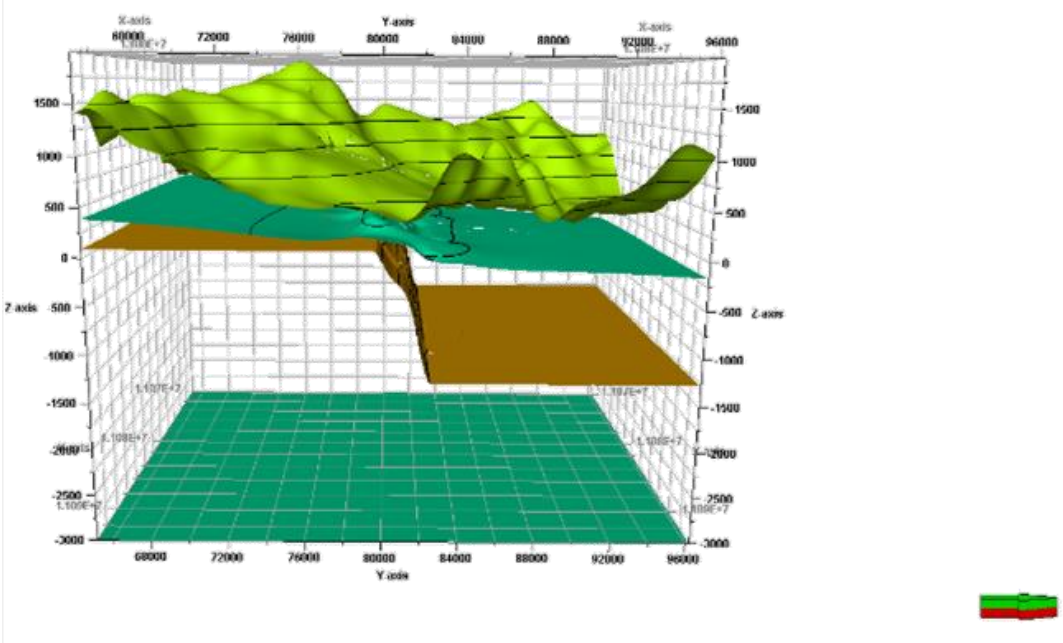

Figure 11: Horizon modeling results

From the structural model, horizon model is created on a skeleton grid with lateral resolution of 50m x 50m. The horizon model was generated using well lithology as main input. The several horizons inside the model represent facies boundary. These boundaries correspond to the tops of Sorik Volcanics, Roburan Volcanics, Sibangor Formation and a bottom layer at -3000m MSL which was assumed as vertical limitation for the model (Figure 11).

Prior to deep exploratory drilling, a 3D stratigraphic model was constructed using gravity data and other third party 3D visualization software. That model was

reconstructed using Petrel® and the result is shown in Figure 12. However, after drilling several deep wells, it was established that the basement was not intersected contrary to initial geological prognosis. It is possible that the basement is too deep and beyond the reach of the exploration wells.

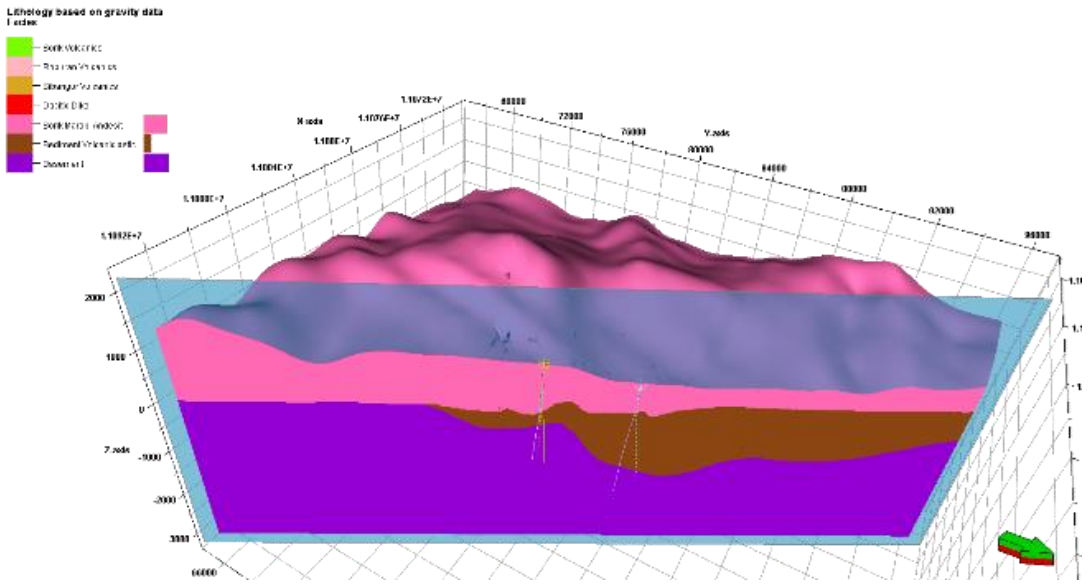

Figure 12: 3D Lithology model based on gravity data from previous study without any well data.

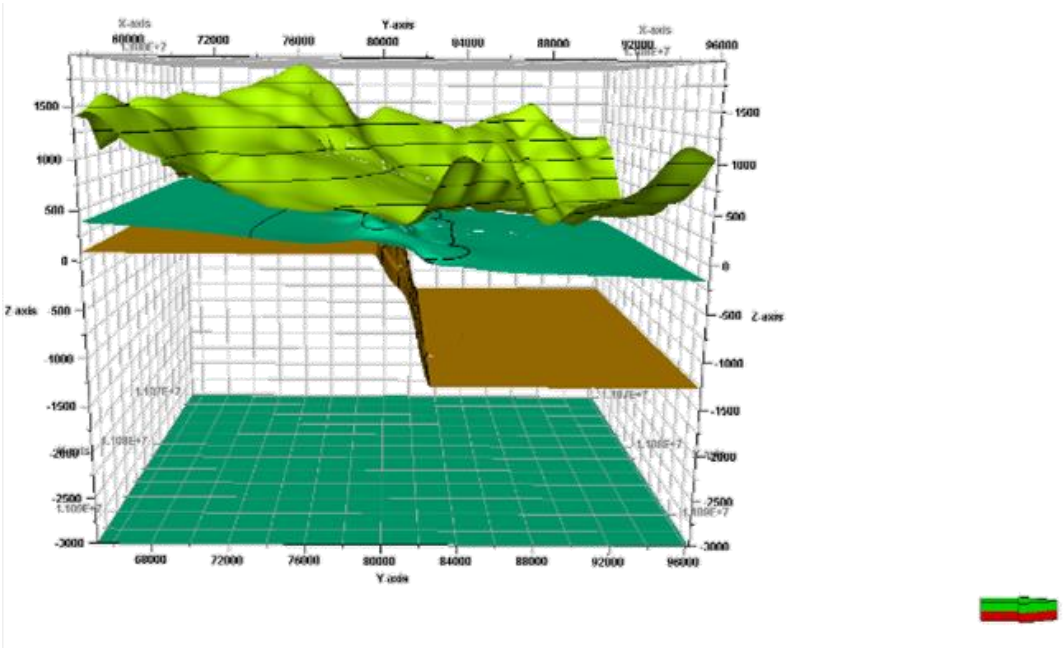

Figure 11: Horizon modeling results

VBased on drill cuttings analyses, the subsurface stratigraphy was remodeled into the 3D grid (Figure 13) and the outcome is quite consistent with the cross-section shown in Figure 3. This model has supported the previous FEDCO (2017) observation that Roburan sector was once a depression where Sibanggor Formation was down thrown and where the bulk of Roburan Volcanics subsequently accumulated. Preponderance of iron hydroxides in cuttings samples implies that volcanics in Roburan was deposited in aqueous environment.

Resistivity Model

For this study, the resistivity distribution data from magnetotelluric (MT) surveys were used in geophysical modeling. The MT measurements were considered as resistivity attributes for point data. The final product of MT data processing is the resistivity distribution in 3D subsurface (Figure 7).

To extract the point data into 3D grid model, the values should be extracted by well log upscaling process. The 3D grid which was previously built consisted of numerous cells where single value can be assigned. In the upscaling process, all values from point data within a cell in 3D grid were assigned as attributes. The cells without any values (due to lack of field measurements) were assigned with values interpolated from neighboring cells. To populate the upscale data for entire 3D grid, petrophysical modeling with kriging method was applied to generate the resistivity model (Figure 14).

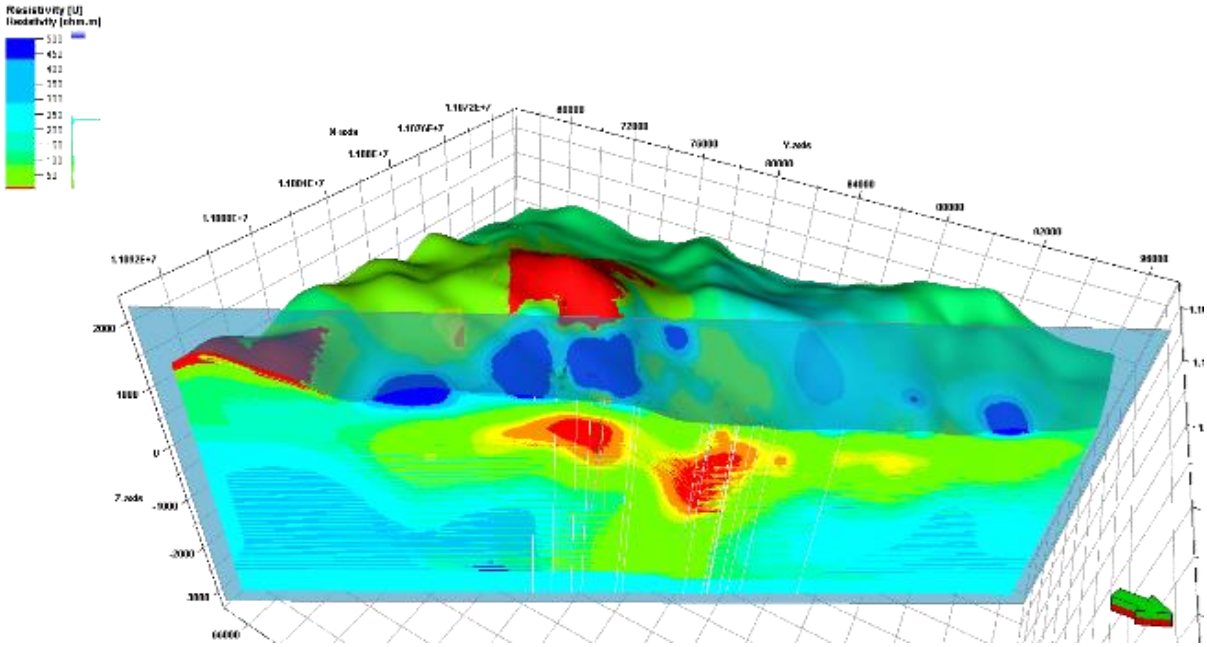

Figure 14: 3D Resistivity model based on points data with resistivity attribute from MT

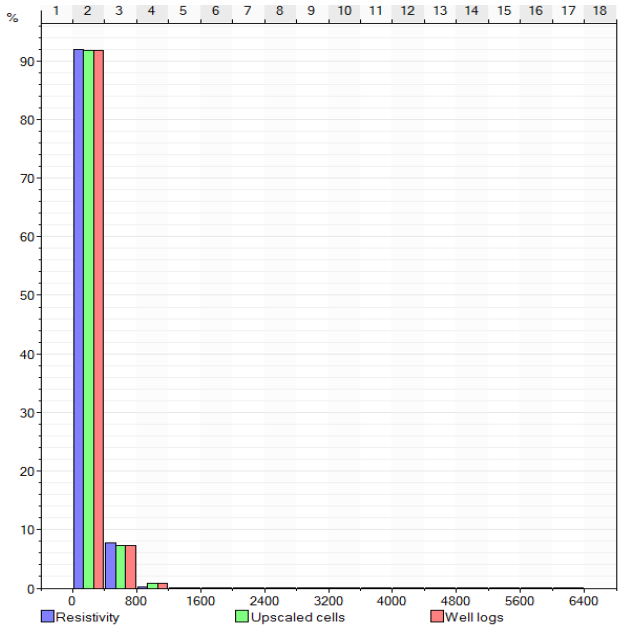

Figure 15: Histogram view which shows the comparison of original data from points, upscaled data and resistivity in the 3D grid model.

This model shows the distribution of resistivity values especially near the wells drilled in pads A and E with characteristic low resistivity. The resistivity value for entire model ranged from1 to 6,300 Ωm.

Quality control for this model was done by checking histogram data of the resistivity model. This histogram showed the comparison between original data, upscaled data and properties model data (Figure 15). Based on the histogram, there was substantial similarity between them which means almost entire value from data has been captured into 3D grid model.

Temperature Model

Being one of the most essential features of a geothermal system, subsurface temperature distribution model is considered as one of the main goals in this study. For this model, temperature data are available from four wells (A102, A103, A104 and E201) that were drilled from pads A and E. The deepest elevation attained by the 4 wells was -1400m MSL. Due to scarcity of data, the best way to model temperature is by using stochastic approach. But the results entail a lot of uncertainties. Thus, temperature modeling was done by deterministic approach similar to resistivity modeling.

The challenge for this method is how to optimize the utilization of available data from the wells to attain a more realistic representation of the resource model. To address this issue, a new attribute for original resistivity point data was created. This new attribute represents the value of temperature at each point. To get that temperature attribute for every point data, the calculator function of Petrel® was applied. This function formula determines the relationship between the measured temperatures of well and resistivity model value at the same location. By plotting Temperature against resistivity, a formula that expresses the relationship between two parameters was generated (Figure 16). Based on the graph, the following equation was derived:

$$y = 202.628 + 0.85288\,x - 0.00265004\,x^2$$

where x =Resistivity(Ωm) and y=Temperature (°C)

Using the above equation, the temperature attributes were established based on resistivity data and used as input for property modeling. The workaround was similar with resistivity modeling previously discussed. Point data attributes were upscaled into 3D grid model, then the values populated into entire grid by doing petrophysical modeling with kriging method. The results show temperatures values ranging from 25°C to 270°C inside the 3D grid model (Figure 17).

Quality control for this model can be done by checking its histogram data similar to what has been done to resistivity model. In addition, well section window was used to compare original temperature data from wells and the resulting model (Figure 18).

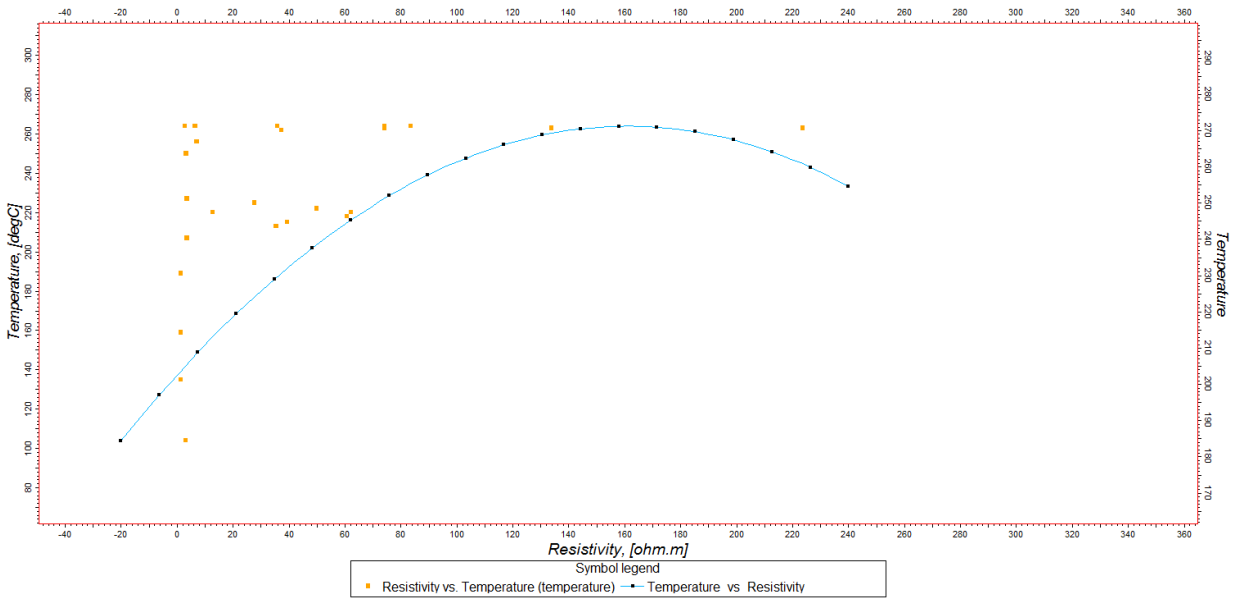

Figure 16: Non-linear function graph generated from resistivity and temperature data relationship.

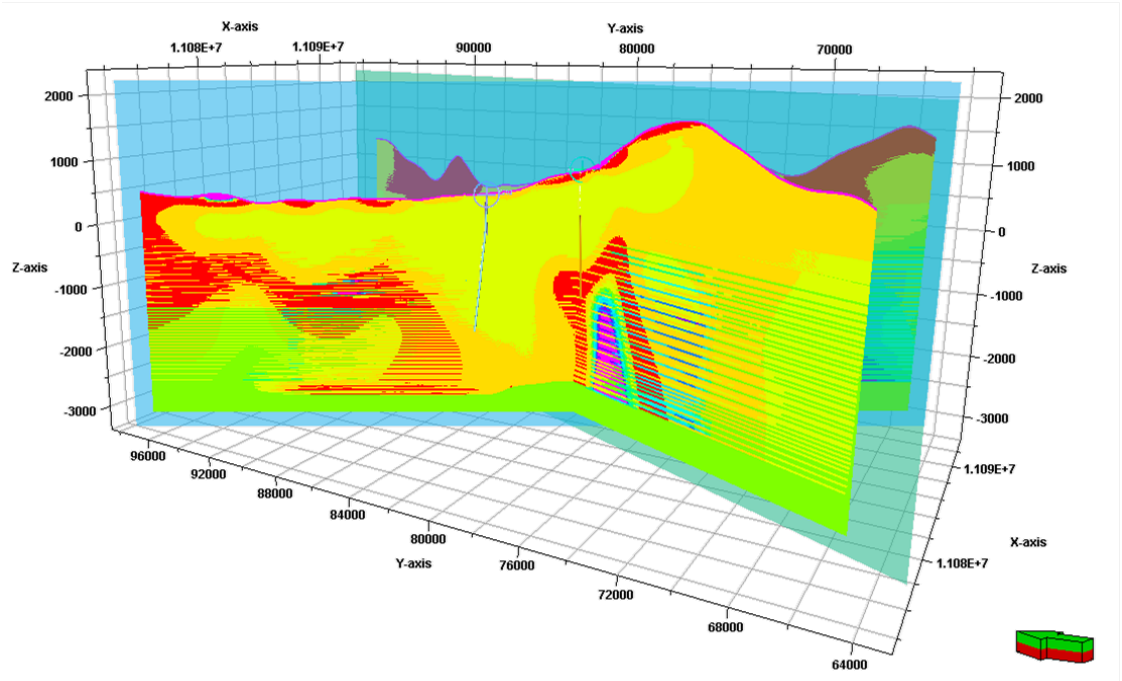

Figure 17: 3D Temperature model based on points data with temperature attributes extracted from resistivity data

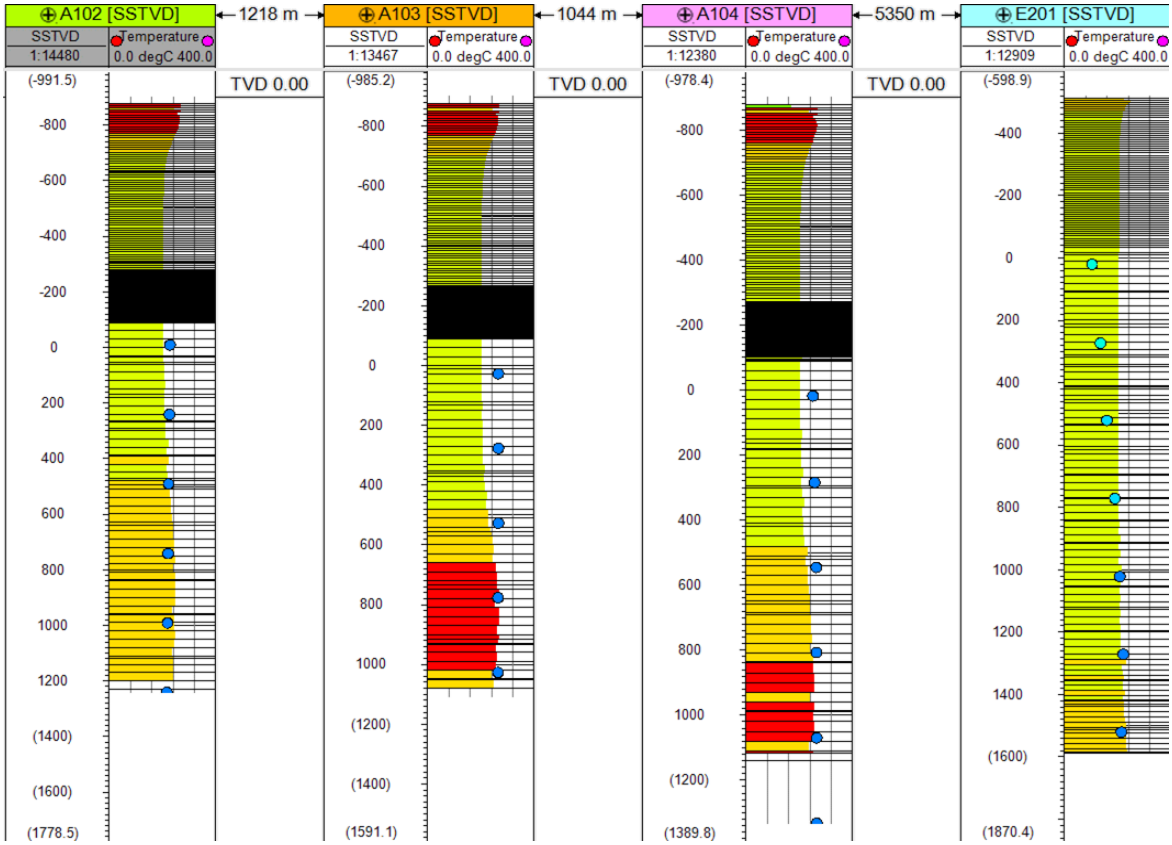

Figure 18: Well section window to compare original well data temperature (blue circle symbol) and result model of temperature

Basing on the 3D visualization and testing at well section window, we can consider that temperature value distribution is reasonably accurate except for locations that were too far from existing wells. It is expected that this temperature model will be improved in the future as more wells are drilled.

DISCUSSION

The model created using the resistivity-derived temperatures demonstrated that the hottest section or the main resource is located in the vicinity of the eastern flank of Mt. Sorik Marapi volcano. The geothermal reservoir is indicated by near vertical feature that may represent the thermal plume emanating from an area beneath Mt. Sorik Marapi. The chimney-like form of the reservoir may have been influenced by scarcity of data at and west of Sorik Marapi volcanic center. It is possible that the size of the resource could even be broader should more MT measurements are conducted within Sorik Marapi volcano and to the west where a large, seemingly ancestral caldera is located.

On the other hand, the model does not clearly define the outflow path of the reservoir nor the possible hydrological connection between the main resource area and the northern chloride springs in Sampuraga area, where the main outflow was previously postulated. The vague hot lateral feature in this sector may denote possible flow path of hot fluids but apparently originating from a different source.

The Model has also shown that the Roburan sector - where wells SME-201 and SME-202 were drilled – is characterized by relatively cold block at the middle of the concession. This area is shown in the model as a possible cold barrier between Sorik Marapi-Sibanggor upflow and Sampuraga chloride hot springs.

CONCLUSIONS

1. The challenges encountered during the modeling processes is the scarcity or even absence of data in some areas. However, the possibility of improving the result model is encouraging, especially when new subsurface data becomes available.
2. 3D subsurface model for the geothermal system was built sequentially from structural model, lithology model, resistivity model and temperature model. Since they are built in the same 3D grid, all of the results should be compatible with each other.
3. This study has shown that, with ample data availability, it is possible to visualize a 3D representation of the geothermal reservoir with reasonable accuracy. This model can be useful for resource assessment, development drilling strategy and future reservoir management.

ACKNOWLEDGEMENTS

The authors would like to thank the managements of KS Orka, PT SMGP and Schlumberger for allowing us to use the data and software in the preparation of this manuscript.

REFERENCES

Akar, S., Atalay, O., Kuyumcul, C., Solarog'lul, U.Z.D., Colpan, B., Arzuman, S., 2011. 3D Subsurface

Modeling of Gümüs¸köy Geothermal Area, Aydın, Turkey. *GRC Transactions*, Vol. 35.

Blanco, D.F., Philippon, M., Hagke, C.V., 2015. Structure and Kinematics of the Sumatran Fault System in North Sumatra (Indonesia). *Tectonophysics*. pp 1-12.

Cattin, R., Chamot-Rooke, N., Pubellier, M., Rabaute, A., Delescluse, M., Vigny, C., Fleitout, L., Dubernet, P., 2009. Stress change and effective friction coefficient along the Sumatra-Andaman-Sagaing fault system after 26 December 2004 (Mw = 9.2) and the 28 March 2005 (Mw = 8.7) earthquakes. *Geochemistry, Geophysics, Geosystems* Vol. 10, Q03011.

Filtech Energy Drilling Company, 2017, Sorik Marapi Geothermal Power Plant ("PLTP Sorik Marapi") 240 MW, Notice of Resources Confirmation, Unpublished Technical Report.

Hamilton, W., 1979. Tectonics of Indonesia Region. *US Geological Survey Professional Paper* 1078. pp. 18-38

Hochstein, M.P., Sudarman, S., 1993. Geothermal resources of Sumatra. *Geothermics Vol. 22*, pp 181–200.

Muraoka, H., Takashi, M., Sundhoro, H., Dwipa, S., Soeda, Y., Momita, M., Shimada, K., 2010. Geothermal systems constrained by the Sumatra Fault and its pull-apart basins in Sumatra, Western Indonesia. In: *Proceedings World Geothermal Congress* – Bali, Indonesia, pp. 1–9.

Petrel*, 2010, Schlumberger Information Solution, Petrel Software Online.

HelpSieh, K., Natawidjaja D., 2000. Neotectonics of Sumatra fault, Indonesia. *Journal of Geophysical Research* Vol. 105, pp. 1-30.

Weller, O., Lange D., Tilmann F., Natawidjaja D., Rietbrock A., Collings R., and Gregory L., 2011. The Structure of the Sumatran Fault revealed by local seismicity. *Geophysical Research Letters*, Vol. 39, pp. 1-7